S. Bechekir, A. Zeghoudi, D. Ould-Abdeslam, M. Brahami, H. Slimani, A. Bendaoud

Development of a boost-inverter converter under electromagnetic compatibility stress equipping a photovoltaic generator

*Introduction. Static converters are among the most widely used equipment in several applications, for example, electric power transmission, motor speed variation, photovoltaic panels, which constitute the electronic components. The design of a power electronics device is done without any real means of predicting electromagnetic disturbances during the product development phase. This case-by-case development process is repeated until a solution is found that best respects all the electromagnetic compatibility constraints. The **purpose** is the development of a boost-inverter converter under electromagnetic compatibility constraints. The improvements made to the inverter are mainly in the control, the choice of power switches and the electromagnetic compatibility solutions brought to the device. The quality of the wave is improved by acting on the type of control and the choice of switches. **Methods.** In the first time, we have highlighted a comparison between two most frequently used power components (MOSFET and IGBT) in the inverter and the boost by simulation using ISIS and LT-spice softwares. The sinusoidal voltage with modulation circuit is greatly simplified by the use of the PIC16F876A microcontroller. In a second step, we validate the obtained results with experimental measurements. We start with the boost, then the inverter. In addition, the circuits made are housed in boxes to avoid accidental contact for people. The equipment is designed to isolate the load from the power supply in case of: over voltages, under voltages, high and low battery level and short circuits. **Results.** All the simulations were performed using the ISIS and LT-spice softwares. The obtained results are validated by experimental measurements performed in the ICEPS Laboratory at the University of Sidi Bel-Abbes in Algeria. The realization of a single-phase inverter with a pulse width modulation control, associated with a boost chopper and the waveforms of the current and voltage across each static converter its opening are presented. The sources of disturbances in power devices are at the origin of the temporal and frequency characteristics of the signals coming from the hot spots of the power switches and the resonances created during the switching of these elements. References 27, figures 23.*
Key words: **inverter, converter, microcontroller, electromagnetic compatibility, MOSFET, IGBT.**

*Вступ. Статичні перетворювачі відносяться до обладнання, що найбільш широко використовується в декількох застосуваннях, наприклад, для передачі електроенергії, зміни швидкості двигуна, у фотогальванічних панелях, які складають електронні компоненти. Проєкт устрою силової електроніки виконується без будь-яких реальних засобів прогнозування електромагнітних перешкод на етапі розробки продукту. Цей процес індивідуальної розробки повторюється доти, доки знайдено рішення, яке найкраще враховує всі обмеження електромагнітної сумісності. **Метою** є розробка підвищувально-інверторного перетворювача при обмеженнях за електромагнітною сумісністю. Удосконалення, внесені в інвертор, в основному стосуються управління, вибору силових вимикачів та рішень щодо електромагнітної сумісності, реалізованих у пристрої. Якість хвилі покращується за рахунок впливу на тип керування та вибір перемикачів. **Методи.** Вперше ми підкреслили порівняння між двома найбільш часто використовуваними силовими компонентами (MOSFET та IGBT) в інверторі та підвищенням шляхом моделювання з використанням програмного забезпечення ISIS та LT-spice. Синусоїдальна напруга зі схемою модуляції значно спрощується за рахунок використання мікроконтролера PIC16F876A. На другому етапі ми підтверджуємо отримані результати експериментальними вимірами. Починаємо з Boost, потім з інвертора. Крім того, виготовлені схеми розміщені в коробках, щоб уникнути випадкового дотику людей. Устаткування призначене для відключення навантаження від джерела живлення у разі: перенапруги, зниженої напруги, високого та низького рівня заряду батареї та короткого замикання. **Результати.** Усі розрахунки проводилися з використанням програм ISIS та LT-spice. Отримані результати підтверджені експериментальними вимірами, проведеними в лабораторії ICEPS Університету Сіді-Бель-Аббес в Алжирі. Представлено реалізацію однофазного інвертора з керуванням на базі широтно-імпульсної модуляції, пов'язаного з підвищуючим переривником, а також осцилограми струму та напруги на кожному відкритті його статичного перетворювача. Джерелами збурень у силових пристроях є часові та частотні характеристики сигналів, що надходять від гарячих точок силових ключів, та резонанси, що створюються при комутації цих елементів.. Бібл. 27, рис. 23.*
Ключові слова: **інвертор, перетворювач, мікроконтролер, електромагнітна сумісність, MOSFET, IGBT.**

Introduction. Electromagnetic compatibility (EMC) is the field of the interactions study that can take place between different devices. It imposes, through standards, constraints in terms of electromagnetic pollution generated by electrical devices (emission standards) and the ability of these same devices to operate in a polluted environment (susceptibility standards) [1].

The integration of EMC issues in the design of converters is quite recent. However, the severity of the standards is such that the measures required to comply with them have a strong impact in terms of cost and size. For example, the traditional interference filtering solution used in inverters and choppers can represent up to a third of their material cost. It is therefore particularly important to take into account the EMC aspect from the product design stage and to look for conversion solutions adapted to this constraint [2].

Inverters are made up of sophisticated, high-performance active and passive components which, however, have a number of limitations that have an impact on the synthesis of control loops [3-8].

Different inverter topologies have been studied with respect to the feasibility of adapting low power ranges at low input voltage to the grid. They can be divided into five categories:

1. Inverter concept with DC voltage link [9, 10]: In order to adapt the photovoltaic (PV) panel voltage to the public grid, DC/DC converters are used. These converters are connected via a DC voltage link to a high-frequency switching converter.

2. Inverter concept with pulsed DC voltage link [11]: these concepts use the same inverters as described in point 1, but their control unit generates the absolute value of a 50 Hz sine wave instead of a DC voltage. This pulsed DC link voltage is inverted by a 50 Hz switching inverter.

3. Inverter concept with AC voltage link [12] DC/DC converters with high frequency transformer, which need a diode rectifier to obtain a DC output voltage; otherwise the output voltage is a bidirectional square wave voltage with the switching frequency as the value. An inverter concept with AC voltage link makes it possible to supply the grid

with this voltage form. Therefore, the inverter needs bidirectional voltage switches.

4. Direct inverter concept: one of these concepts includes a high frequency switched inverter connected to a 50 Hz transformer. The other concept is a transformer less topology that includes 2 bidirectional inverters in parallel series connection [13, 14].

5. Pulsed DC link using a resonant converter: this is the same inverter concept as described in 2. However, instead of a series of parallel DC/DC converters or resonant converters, the converters are connected to the link [15, 16].

Switching is provided by power switches based on semiconductors. There are 2 types of switches with controlled switching (MOSFET, IGBT, thyristor and so on) with rapid variation the voltage or current as function of time, and others with uncontrolled switching (diodes), which generate harmonic distortion and low power factor [17-20].

Goal. In this paper, we characterize by simulation the different switches and we observe their impacts on the chopper and the inverter. We will choose the least disturbing switch. Moreover, we use 2 control techniques of the inverter in order to compare the spectrum of the output voltage. The objective is to be able to evaluate the EMC impact of the inverter during the design phase.

Structure of the proposed PV inverter. Figure 1 shows the general structure of the proposed PV system, which is presented in the form of 2 blocks: the boost part and the inverter part.
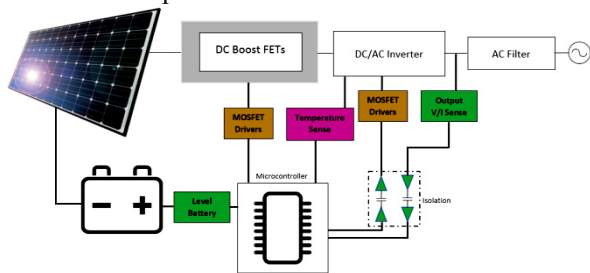

Fig. 1. Functional diagram of the inverter

The block diagram of the PV converter developed with the ISIS software consists inverter control part (Fig. 2), power part (Fig. 3) DC boost (Fig. 4). The inverter features input voltage protection, output voltage and current regulation, and switch overheating protection.
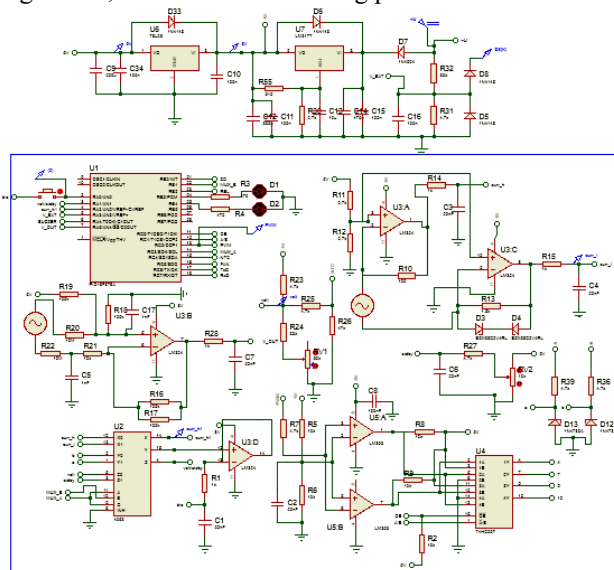

Fig. 2. Inverter control part in the developed PV converter circuit
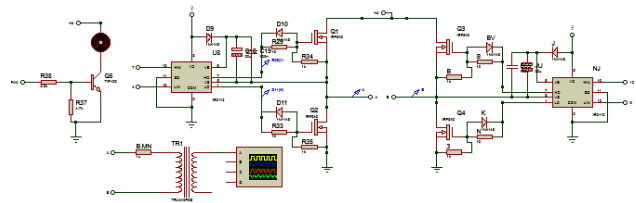
Fig. 3. Power part in the developed PV converter circuit
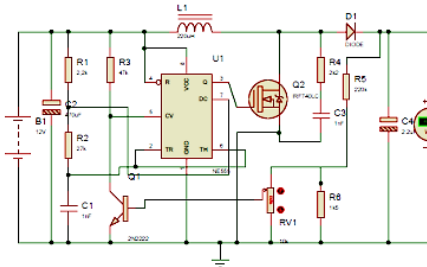
Fig. 4. DC boost in the developed PV converter circuit

Choice of switches. For the design of the boost and the inverter, there are 2 main types of switches used in power electronics: the power MOSFET, which looks very similar to a standard MOSFET, but it is designed to handle relatively large voltages and currents. The other component is the IGBT [14]. The specifications of the 2 switches overlap to a large extent.

Power MOSFETs have a much higher switching frequency capability than IGBTs and can be switched at frequencies above 200 kHz. They don't have the same capability for high-voltage, high-current applications, and tend to be used at voltages below 250 V and powers below 500 W. Both of MOSFETs and IGBTs have power losses due to the rise and fall of the voltage on and off (dV/dt losses). Unlike IGBTs, MOSFETs have a body diode.

As a general rule, IGBTs are the ideal solution for high-voltage, low-frequency applications (> 1000 V and < 20 kHz) and MOSFETs are ideal for low-voltage, high-frequency applications (< 250 V and > 200 kHz) [21]. Between these 2 extremes, there is a large gray area. In this area, other considerations such as power, duty cycle percentage, availability and cost tend to be the deciding factors.

To highlight the effects of the switches, the boost setup was analyzed by simulation with the LT-spice software. Three different IGBT switches (IRGBC20U, IRGBC30U and IRGBC40U) and 3 different MOSFET switches (IPB65R110CFD, R6020ANX and STW11NM80) were used in this work. The 3 selected IGBTs and 3 MOSFETs were tested by simulation during their operation in the boost and inverter, to compare the EMC disturbances generated by the different types of switches. The obtained results for the boost are shown in Fig. 5, 6, and for inverter parts – in Fig. 7, 8.
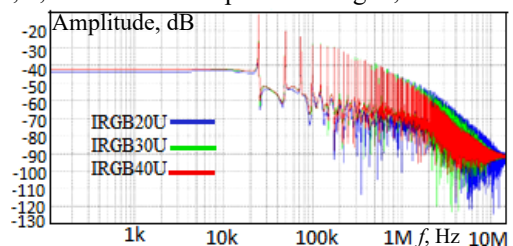
Fig. 5. Comparison of the boost voltages between the 3 IGBTs in frequency domain
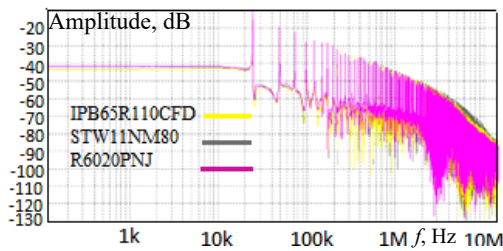
Fig. 6. Comparison of the boost voltages between the 3 MOSFETs in frequency domain
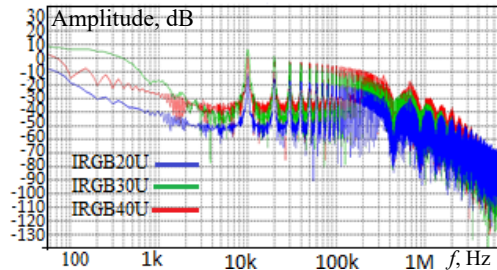
Fig. 7. Comparison of the inverter voltages between the 3 IGBTs in frequency domain
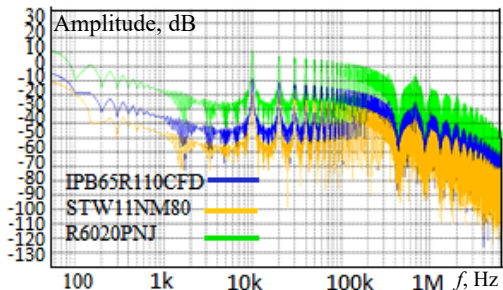

Fig. 8. Comparison of the inverter voltages between the 3 IGBTs in frequency domain

Figures 5, 6 present the spectra of the frequency variation of boost for 3 types of switches IGBT and MOSFET respectively. We can see that the spectrum of the IGBT IRGBC40U tends to decrease regularly and more quickly from 1 MHz. For the 3 MOSFETs the spectrum of R6020ANX tends to decrease compared to the others from 3MHz.

Figures 7, 8 present the spectra of the frequency variation of the inverter for 3 types of switches IGBT and MOSFET respectively. We can see that the spectrum of the IGBT IRGBC20U decreases regularly and in a less important way from 2 MHz. For the 3 MOSFETs the spectrum of STW11NM80 is lower than the others.

An analysis was performed to compare between the IGBT and the MOSFET with the least disturbance determined below. The results of the comparative analysis between the 2 types of switches are shown in Fig. 9, 10 for the boost and inverter respectively.
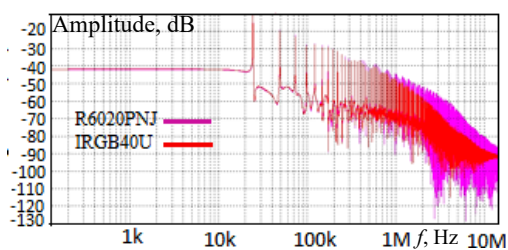
Fig. 9. Comparison of frequency analysis between IGBT and MOSFET in the case of boost
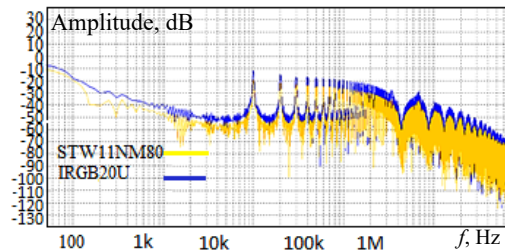
Fig. 10. Comparison of frequency analysis between IGBT and MOSFET in the case of inverter

Figures 9, 10 present a comparison of the frequency analysis between the IGBT and the MOSFET at the boost level and the inverter respectively. We can see that the spectrum of the IGBT IRGBC40U tends to decrease regularly and more quickly from 1 MHz. So, at the boost level the IGBT is the least disturbing. At the inverter level, the MOSFET STW11NM80 is the least disturbing switch with a difference of 8 dB compared to the IGBT.

Choice of the control type. A pulse width modulation (PWM) law results from the comparison of 2 modulators with a carrier. The implementation of this principle is shown in Fig. 11 [22-25].
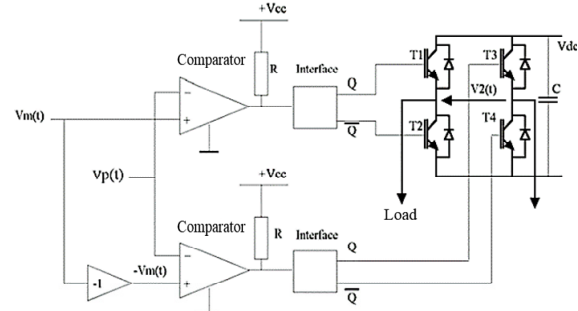

Fig. 11. Principle of generation of a unipolar PWM law with frequency doubling

The second law of PWM results from the comparison of 2 carriers with a modulator. The implementation of this principle is shown in Fig. 12 [13].
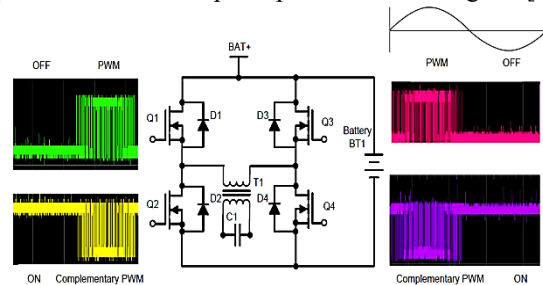
Fig. 12. Principle of PWM generation

For the positive half of the sine wave generation, Q2 is always on, Q1 is always off, Q3 is applied with 20 kHz PWM corresponding to positive half cycle 50 Hz sine wave and Q4 is applied with corresponding complementary (to Q3) PWM. For the negative half 50 Hz sine wave generation, Q4 is always high, Q3 is always off, Q1 is applied with 20 kHz PWM corresponding to positive half cycle 50 Hz sine wave and Q2 is applied with Q1 complementary PWM.

We apply these 2 commands to the inverter. The frequency analysis of the inverter is given in Fig. 13.

Figure 13 presents the frequency analysis of the inverter with the 2 commands. It can be seen that the control spectrum with the two-carrier impulse modulation

law is the least disturbing. The spectrum decreases regularly and more rapidly from 20 kHz with a difference of 5 dB compared to that of 2 modulators with one carrier.
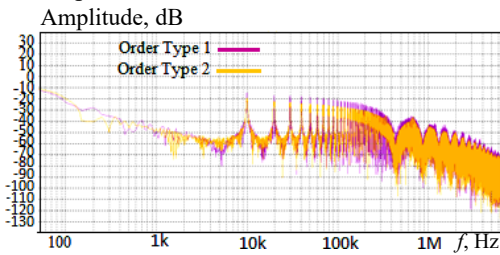

Fig. 13. Frequency analysis of the inverter with the 2 commands

Protection of the inverter. There are many feedback signals at the input of the microcontroller necessary for the proper operation of the inverter, we cite:

- input voltage sensor (battery);
- temperature sensor (R_t, negative temperature coefficient (NTC) –47 K) of electronic switches;
- AC output current and voltage sensor (230 V).

The current, which is the main source of heating, considerably reduces the efficiency of the inverter and can damage it. For this reason, a forced cooling is implemented to obtain a better efficiency. The control block diagram used is shown in Fig. 14.
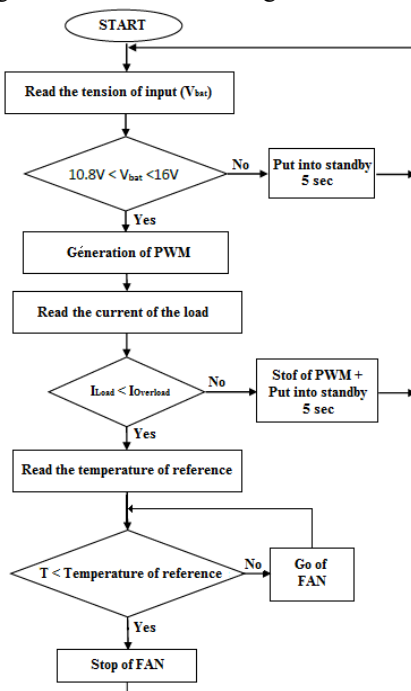

Fig. 14. Algorithm of control

MOSFET driver. It is advantageous to use N-channel MOSFETs as switches because they have a low on-resistance [26]. This results in low power losses. However, to do this, the drain of the high-side switch is connected to a 340 V DC supply converted to 240 V AC. The voltage at the gate terminal must be 10 V higher than that at the drain terminal [10, 14]. Therefore, to drive the H-bridge MOSFETs, a bootstrap capacitor designed specifically to drive a half-bridge is used. After considering different integrated circuit options, our choice was the IR2113. It is supplied by a 600 V rating, 2 A drive current, and a 10-20 V drive voltage. The activation and deactivation times are respectively 120 ns and 94 ns [23, 24].

We implemented the control routine in a programmable interface controllers (PIC) PIC16F876A microcontroller and configured the analog/digital conversion module integrated in this circuit, to automatically start the conversion.

The MOSFET driver is actuated by a signal delivered by the microcontroller. It is supplied by the battery. The driver is able to control the switches. The upper high side switch requires an additional voltage of 10 V. This is achieved by an external bootstrap capacitor charged by a diode from the 12 V supply when the device is off [27].

Obtained results. No-load test. Figures 15, 16 show the generation of the PWM. Figure 17 shows the output voltage signals from the inverter.
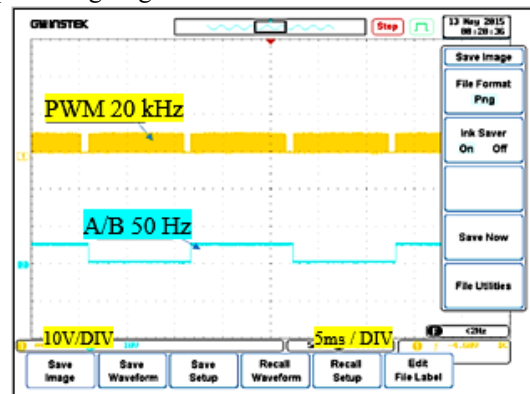
Fig. 15. PWM and A/B peak output
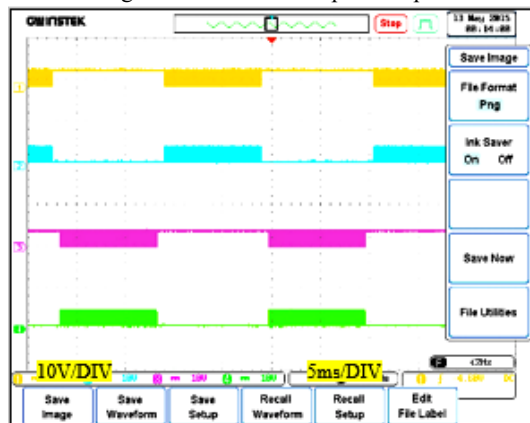

Fig. 16. 74HC257 output signal
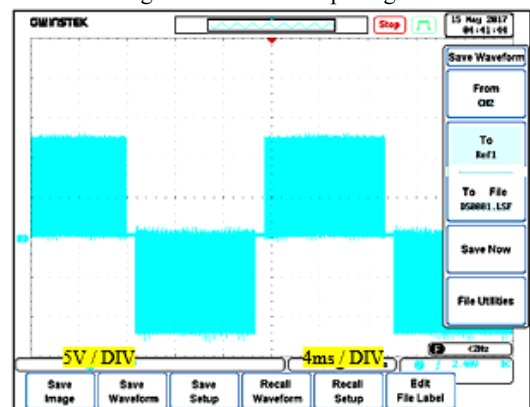
Fig. 17. Voltage at the output of the inverter (no-load test)

At a high temperature of the switches (MOSFET), the NTC heats up and gives the order to the PIN FAN to generate the signal to start the fan. At a very high temperature the microcontroller blocks the generation of the PWM. This stops the inverter. The fan runs until the switches cool down.

Boost mounting tests. Boost chopper is supplied by a 12 V voltage. The output voltage is adjustable by a potentiometer up to 340 V. Figure 18 shows the curve of the boost voltage.
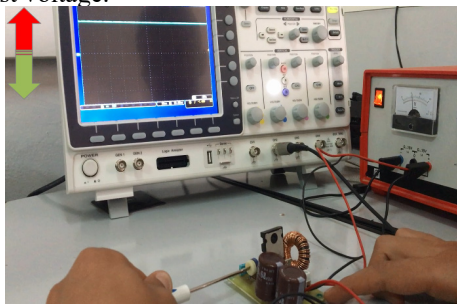

Fig. 18. Boost test at 12 V input voltage

The inverter test is shown in Fig. 19. Figure 20 shows the voltage delivered by the inverter.
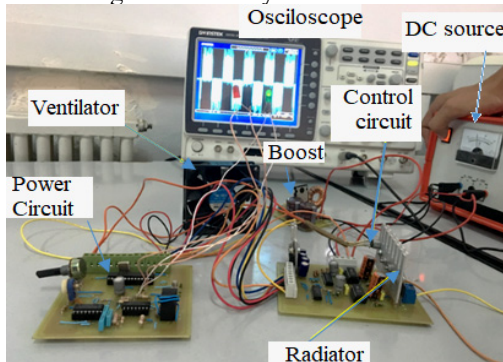

Fig. 19. Complete circuit (power part and inverter and boost control)
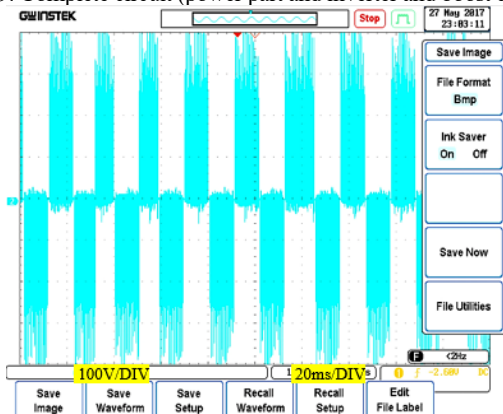
Fig. 20. Voltage at the output of the inverter (boost mounting tests)

Load test. The inverter feeds an inductive load consisting of a 100 Ω resistor and a 1 H coil (internal resistance of about 12 Ω). The voltage and current are shown in Fig. 21, 22.
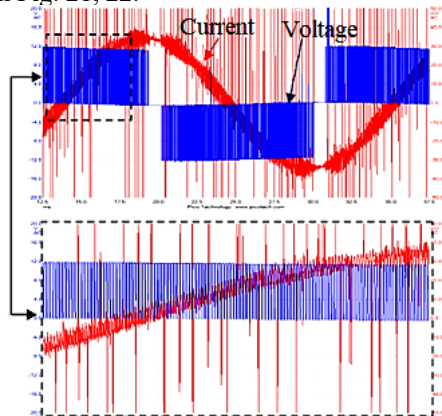

Fig. 21. Inverter output current and voltage signal
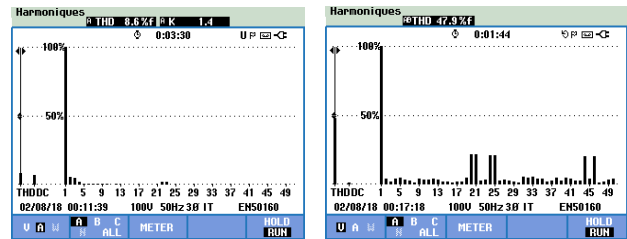
Fig. 22. Voltage/current spectrum for a modulation index $m = 0.9$

Enclosure and circuit location. The inverter boards are placed in suitable positions. A shielding technique is used. The separation of the power and control circuits is made by grids as shown in Fig. 23 in order to reduce the coupling between the circuits by electromagnetic radiation.

The LEDs L1, L2, signal the status of the inverter:
- L1 (green) → power on;
- L2 (red) → battery low (< 10 V);
- L1 (green) flashing → standby mode;
- L2 (red) flashing → high temperature of power transistors.

Voltage spikes. When the driver is used to drive an inverter with inductive load impedance, it can develop voltage spikes due to reverse voltages. These spikes can damage the MOSFETs and their control circuits. For this reason, integrated diode transistors have been used to conduct strongly as soon as the voltage increases excessively, thus protecting the MOSFETs.

Capacitive load. Since this inverter is a quasi-sine wave type, high frequency harmonics have been completely eliminated. When used with a capacitive load, the impedance is exactly as calculated. The problem with other types of inverters is that, due to high frequency harmonics, the capacitive impedance decreases, which implies an increase of the current beyond the nominal value.
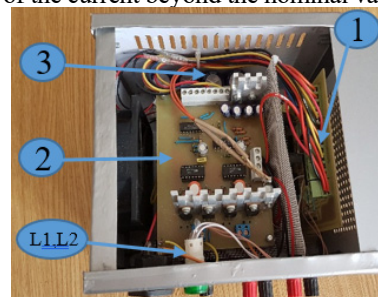
Fig. 23. Internal views of the realized inverter box:

1 – control circuit;
2 – power circuit;
3 – boost

Conclusions.

1. The rise and fall time as well as the switching frequency are very important factors to characterize a useful signal in the field of power electronics. We have highlighted a comparison between two most frequently used power components (MOSFET and IGBT) in the inverter and the boost.

2. We have studied the behavior of semiconductor components in the frequency domain generating a high harmonic number located in the high frequency region. The spectra have different amplitudes due to the difference between the intrinsic characteristics of each switch. Therefore, each power switch has its own electromagnetic compatibility signature.

3. The sinusoidal voltage with modulation circuit is greatly simplified by using the PIC16F876A microcontroller. In addition to the high programming flexibility, the switching pulse design can be changed without further hardware modification. The inverter is shielded against radiated electromagnetic interference. This increases its efficiency.

4. The realization of a single-phase inverter with PWM control, associated with a boost chopper; and this circuit are

housed in enclosures to avoid accidental contact with people. The equipment is designed to isolate the load from the power supply in case of: overvoltages, undervoltages, high and low battery levels and short circuits.

Conflict of interest. The authors declare that they have no conflicts of interest.

REFERENCES

1. Kimmel W.D., Gerke D. *Electromagnetic compatibility in medical equipment: a guide for designers and installers*. CRC Press, 2019. 302 p.
2. Lee F.C., Daan Van Wyk J., Boroyevich D., Barbosa P. An integrated approach to power electronics systems. *Proceedings of the Power Conversion Conference-Osaka 2002 (Cat. No.02TH8579)*, Osaka, Japan, 2002, vol. 1, pp. 7-12. doi: https://doi.org/10.1109/PCC.2002.998503.
3. Song Y., Wang B. Survey on Reliability of Power Electronic Systems. *IEEE Transactions on Power Electronics*, 2013, vol. 28, no. 1, pp. 591-604. doi: https://doi.org/10.1109/TPEL.2012.2192503.
4. Rahim N.A., Selvaraj J. Multistring Five-Level Inverter With Novel PWM Control Scheme for PV Application. *IEEE Transactions on Industrial Electronics*, 2010, vol. 57, no. 6, pp. 2111-2123. doi: https://doi.org/10.1109/TIE.2009.2034683.
5. Barrade P. *Power Electronics: Converters Methodology and Elementals*. Lausanne Polytechnic and University Presses Romandes, First Edition, 2006.
6. Buttay C. *Contribution to Conception by Simulation in Power Electronics. Application to the inverter Low Voltage*. National Institute of Applied Sciences, Lyon, November 2004.
7. Hasan M., Maqsood J., Baig M.Q., Bukhari S.M.A.S., Ahmed S. Design and Implementation of Single Phase Pure Sine Wave Inverter Using Multivibrator IC. *2015 17th UKSim-AMSS International Conference on Modelling and Simulation (UKSim)*, 2015, pp. 451-455. doi: https://doi.org/10.1109/UKSim.2015.58.
8. Haeberlin H. Evolution of Inverters for Grid connected PV-Systems from 1989 to 2000. *17th European Photovoltaic Solar Energy Conference*, Munich, Germany, 2001, 5 p.
9. Koutroulis E., Chatzakis J., Kalaitzakis K., Voulgaris N.C. A bidirectional, sinusoidal, high-frequency inverter design. *IEE Proceedings - Electric Power Applications*, 2001, vol. 148, no. 4, pp. 315-321. doi: https://doi.org/10.1049/ip-epa:20010351.
10. Thukral R., Kumar G., Gupta A., Kumar Verma N., Asthana S. Microcontroller Based Solar Power Inverter. *International Journal of Electrical Engineering & Technology (IJEET)*, 2016, vol. 7, no. 5, pp. 70-78.
11. Bechekir S., Bousmaha I.S., Brahami M., Abdeslam D.O. Realization of an inverter with PWM command for photovoltaic system. *2017 5th International Conference on Electrical Engineering - Boumerdes (ICEE-B)*, 2017, pp. 1-6. doi: https://doi.org/10.1109/ICEE-B.2017.8192003.
12. Aganza T.A., Pérez R.J., Beristain J.J.A. Inversor trifásico SPWM para el control de velocidad de un motor de inducción implementado en el microcontrolador PIC18F2431. *Revista de Ingeniería Eléctrica, Electrónica y Computación*, 2006, vol. 2, no. 1, pp. 7-16. (Esp).
13. Dixit S., Tripathi A., Chola V., Verma A. *800VA Pure Sine Wave Inverter's Reference Design*. Texas Instruments. Application Report SLAA602A, June 2013 (Revised August 2017).
14. Mamun A.A., Elahi M.F., Quamruzzaman M., Tomal M.U. Design and implementation of single phase inverter. *International Journal of Science and Research (IJSR)*, 2013, vol. 2. no. 2, pp. 163-167.
15. Chuang Y.-C., Ke Y.-L., Chuang H.-S., Chen J.-T. A Novel Loaded-Resonant Converter for the Application of DC-to-DC Energy Conversions. *IEEE Transactions on Industry Applications*, 2012, vol. 48, no. 2, pp. 742-749. doi: https://doi.org/10.1109/TIA.2011.2180875.
16. Tseng S.-Y., Wang H.-Y. A Photovoltaic Power System Using a High Step-up Converter for DC Load Applications. *Energies*, 2013, vol. 6, no. 2, pp. 1068-1100. doi: https://doi.org/10.3390/en6021068.
17. Zeghoudi A., Slimani H., Bendaoud A., Benazza B., Bechekir S., Miloudi H. Measurement and analysis of common and differential modes conducted emissions generated by an AC/DC converter. *Electrical Engineering & Electromechanics*, 2022, no. 4, pp. 63-67. doi: https://doi.org/10.20998/2074-272X.2022.4.09.
18. Muttaqi K.M. Electromagnetic Interference Generated from Fast Switching Power Electronic Devices. *International Journal of Innovations in Energy Systems and Power*, 2008, vol. 3, no. 1, pp. 19-26.
19. Slimani H., Zeghoudi A., Bendaoud A., Reguig A., Benazza B., Benhadda N. Experimental Measurement of Conducted Emissions Generated by Static Converters in Common and Differential Modes. *European Journal of Electrical Engineering*, 2021, vol. 23, no. 3, pp. 273-279. doi: https://doi.org/10.18280/ejee.230312.
20. Zeghoudi A., Bendaoud A., Slimani H., Benazza B., Bennouna D. Determination of electromagnetic disturbances in a buck chopper. *Australian Journal of Electrical and Electronics Engineering*, 2022, vol. 19, no. 2, pp. 149-157. doi: https://doi.org/10.1080/1448837X.2021.2023073.
21. Bechekir S., Brahami M., Ould Abdeslam D., Nemmich S., Nassour K., Tilmatine A. Development of a Low-Cost Ozone Generator Supply-Optimization Using Response Surface Modeling. *International Journal of Plasma Environmental Science and Technology*, 2019, vol. 13, no. 1, pp. 7-13. doi: https://doi.org/10.34343/ijpest.2019.13.01.007.
22. Leung H.F., Crowley I.F. *PWM Techniques: A Pure Sine Wave Inverter*. Worcester Polytechnic Institute, Major Qualifying Project, 2011.
23. IR2110/IR2113. *Data Sheet No. PD60147-L*. IOR International Rectifier, 2003.
24. *HV Floating MOS-Gate Driver ICs. Application Note AN-978*. IOR International Rectifier, 2003.
25. Baazouzi K., Bensalah A.D., Drid S., Chrifi-Alaoui L. Passivity voltage based control of the boost power converter used in photovoltaic system. *Electrical Engineering & Electromechanics*, 2022, no. 2, pp. 11-17. doi: https://doi.org/10.20998/2074-272X.2022.2.02.
26. Janardhan G., Surendra Babu N.N.V., Srinivas G.N. Single phase transformerless inverter for grid connected photovoltaic system with reduced leakage current. *Electrical Engineering & Electromechanics*, 2022, no. 5, pp. 36-40. doi: https://doi.org/10.20998/2074-272X.2022.5.06.
27. Parimalasundar E., Kumar N.M.G., Geetha P., Suresh K. Performance investigation of modular multilevel inverter topologies for photovoltaic applications with minimal switches. *Electrical Engineering & Electromechanics*, 2022, no. 6, pp. 28-34. doi: https://doi.org/10.20998/2074-272X.2022.6.05.

Seyf Eddine Bechekir[1], *Lecturer,*
Abdelhakim Zeghoudi[2], *PhD,*
Djaffar Ould-Abdeslam[3], *Professor,*
Mostefa Brahami[1], *Professor,*
Helima Slimani[4], *Lecturer,*
Abdelber Bendaoud[2], *Professor,*
[1] Intelligent Control and Electrical Power Systems (ICEPS),
Djillali Liabes University of Sidi Bel-Abbes, Algeria,
e-mail: seyfeddine.electrotechnique@gmail.com;
mbrahami@yahoo.com
[2] Laboratory of Applications of Plasma, Electrostatics and Electromagnetic Compatibility (APELEC),
Djillali Liabes University of Sidi Bel-Abbes, Algeria,
e-mail: hakooumzeghoudi@gmail.com;
babdelber@gmail.com (Corresponding Author)
[3] MIPS Laboratory,
Universite de Haute Alsace, Mulhouse, France,
e-mail: djaffar.ould-abdeslam@uha.fr
[4] University of Tiaret, Algeria,
e-mail: halima.slimani@univ-tiaret.dz